N89-23906

TRACTION-DRIVE FORCE TRANSMISSION FOR TELEROBOTIC JOINTS*

D. M. Williams** and D. P. Kuban**

ABSTRACT

The U.S. Space Station Program is providing many technological developments to meet the increasing demands of designing such a facility. One of the key areas of research is that of telerobotics for space station assembly and maintenance. Initial implementation will be with teleoperated devices, but long-term plans call for autonomous robotics. One of the essential components for making this transition successful is the manipulator joint mechanism.

Historically, teleoperated manipulators and industrial robotics have had very different mechanisms for force transmission. This is because the design objectives are almost mutually exclusive. A teleoperator must have very low friction and inertia to minimize operator fatigue. Backlash and stiffness are of secondary concern. A robot, however, must have minimum backlash, and high stiffness for accurate and rapid positioning. A joint mechanism has yet to be developed that can optimize these divergent performance objectives.

A joint mechanism that approaches this optimal performance was developed for NASA Langley Research Center, Automation Technology Branch. It is a traction-drive differential that uses variable preload mechanisms. The differential provides compact design, with dexterous motion range and torque density similar to geared systems. The traction drive offers high stiffness and zero backlash for good robotic performance. The variable-loading mechanism (VLM) minimizes the drive-train friction for improved teleoperation. As a result, this combination provides a mechanism to allow advanced manipulation with either teleoperated control or autonomous robotic operation. This paper will address the design principles of both of these major components of the joint mechanism. Also, various surface modifications to these rollers were studied utilizing previous NASA Lewis Research Center experience. For the VLM, several designs were fabricated and tested to optimize operational performance. Test results from the test joints are included. At the time of this writing, final assembly is under way. Finally, the paper describes some of the limitations of this mechanism, as well as recommendations for further development of this technology.

---

*Research sponsored by NASA Langley Research Center under Interagency Agreement Number 40-1553-85 with Martin Marietta Energy Systems, Inc.

**Oak Ridge National Laboratory, Oak Ridge, Tennessee 37831-6353.

INTRODUCTION

The purpose of developing a telerobotic work package for space application is to increase astronaut and overall system safety, productivity, and flexibility. Astronaut safety is of increasing concern because of the number of potentially hazardous tasks, such as hydrazine fuel transfer, being planned for space execution. Astronaut risks increase as the demand for extra vehicular activity (EVA) time increases for work on large projects such as space station assembly, operation, and maintenance activities. A remote system would allow around-the-clock operation while the astronaut-operators remain safely inside the orbiter or space station. Finally, with a telerobotic-based dexterous remote-handling system, operations in the far future can be conducted at significant distances (such as geosynchronous orbit) from the orbiter or space station.

The basic criteria for this telerobotic work package are very straightforward. First, the telerobot must replace the dexterity of a suited astronaut, while allowing the operator to work remotely in a "shirt-sleeves" environment. In addition, the design must allow for the transition from near-term teleoperation to far-term autonomous robotic operation.

Traditionally, teleoperated manipulators have been designed primarily for low friction and inertia to minimize operator fatigue. Backlash and stiffness were of secondary concern. Robots, on the other hand, are designed with high stiffness and minimum backlash as a primary concern to accommodate accurate and rapid positioning. Friction and inertia are addressed secondarily, if at all. The design objectives of teleoperators and robots dictate mechanical approaches that are almost mutually exclusive. Attempts to merge these technologies into a "telerobot" have been strictly limited by these contradictory approaches. To accomplish this merger, a joint mechanism is needed that provides very low friction and inertia to accommodate teleoperator requirements and high stiffness and zero backlash to accommodate robotic requirements. A joint mechanism has yet to be developed that can optimize all of these requirements. However, a joint mechanism that approaches this optimal performance has been developed for NASA Langley, Automation Technology Branch called the Laboratory Telerobotic Manipulator (LTM). It consists of a traction drive differential that uses VLMs.

TRACTION-DRIVE JOINT MECHANISM FOR THE LTM

The LTM is a 7-degree-of-freedom (DOF) telerobot that employes replicated traction drive joint mechanisms as shoulder, elbow, and wrist joints (Fig. 1). Each joint mechanism provides pitch and yaw motions about orthogonal axes. Each joint is attached to the adjacent joints by means of only four fasteners to produce a modular mounting arrangement that allows the LTM arms to be easily assembled and disassembled. This modularity also allows the LTM arms to be easily reconfigured for changing requirements and permits maintenance on the arms by simple module replacement.

The LTM has load capacities to accommodate man-equivalent operation. Each LTM arm has a peak load capacity of 30 lb and a continuous load capacity of 20 lb. To accomplish this requirement effectively, the LTM arm was configured by joints having different torque capacities. The resulting torque requirement for each joint is 435 in.-lb for the wrist, 960 in.-lb for the elbow, and 1650 in.-lb for the shoulder. To reduce the fabrication and engineering cost, a large joint having a peak torque capacity of 1650 in.-lb is used at both shoulder and elbow positions. In an effort to optimize dexterity and minimize weight, a small joint having a peak torque capacity of 435 in.-lb is used as the wrist joint. An assembly of the small joint is illustrated in Figure 2. The large joint is simply an enlarged replica of the small joint and is illustrated in Figure 3. Both joint assemblies consist of a differential drive mechanism, two dc servomotors (Inertial Motors) with gearheads, two torque sensors, and two resolvers as shown in Figures 2 and 3. The speed-reduction ratio through the differential is $\sim$ 3-1/2 to 1. Special gearhead (Bayside Controls) with spring-loaded antibacklash gear trains were used. Commercially available (GSE) torque sensors have been modified and incorporated directly into the joint mechanism to produce a compact arrangement. Vernitron resolvers are located at each joint axis and are coupled directly to the axis of rotation. These resolvers and torque sensors provide the control system data indicating the joint's payload and position.

Cabling provisions have also been made to eliminate the use of external pigtails and connectors. A through-passage within the differential has been provided to accommodate the cabling bundle. This cabling bundle is also equipped with electrical connectors positioned at each mounting interface that engage and disengage automatically as each joint is attached and detached to the adjacent joint.

Permanent-magnet fail-safe brakes have recently become commercially available (Electroid). These brakes have been coaxially mounted to each drive motor and will safely stop each LTM arm during power failure and provide the capability of supporting maximum payloads for long periods without motor overheating. The operating principle of a permanent-magnet brake is similar to that of a standard spring-set brake in the sense that permanent magnets are used to generate a magnetic force that replaces the spring force of the spring-set-type brakes. When the coil of a permanent magnet brake is energized, it cancels this magnetic force, releasing the clamping force on the drive disc. The real advantage of these brakes is their high torque capacity per unit size and weight. These magnetic units are capable of supplying five times the torque-to-weight ratio as spring-set brakes.

The differential drive mechanism has two inputs and one output which rotate about orthogonal axes. Force transmission through the differential drive mechanism is accomplished by traction drives. Unlike force transfer through gear teeth that generate torsional oscillation as the load transfers between teeth, force transfer through traction is inherently smooth and steady, without backlash, and is also relatively stiff [1]. The elements of this traction differential drive can be seen in Figure 4. Two driving rollers provide input into the differential. A significant advantage in this setup is

that each driving roller is required to transmit only one-half of the total torque necessary to make a particular motion. These rollers drive two intermediate roller assemblies, which in turn drive the pitch/yaw roller about the pitch and yaw axes. The axis about which the pitch/yaw roller rotates depends on the direction of rotation of the driving rollers. The pitch/yaw roller is driven about the pitch axis when the driving rollers rotate in the opposite direction. When both driving rollers are rotated in the same direction, the pitch/yaw roller is driven about the yaw axis. Vernitron resolvers are located at each joint axis in an effort to maximize positioning accuracy. By locating these resolvers directly at each joint axis, any creep events that occur through the traction drive differential will not effect the positioning characteristics of the LTM.

The rolling surfaces of the differential are gold plated in an ion-plating process recommended by NASA Lewis Research Center [2]. This plating serves as a dry lubricant that prevents the rolling base materials from contacting. The ion-plating process was performed in a "TORUS 10 MAGNETRON" plating chamber. Each traction drive roller was sputter cleaned in the plating chamber before plating. This was accomplished by evacuating the chamber to 5×10^{-5} Torr, backfilling it with argon to 12×10^{-3} Torr and applying 2000 V negative potential to each roller for 10 min. After sputter cleaning, each roller was plated at a deposition rate of 10Å per second for approximately 3 minutes until a total thickness of 2000 Å was reached.

VLMs have also been employed as an alternative to constant-loading mechanisms in an effort to improve the differentials back-driveability, mechanical efficiency, and fatigue life. Constant-loading mechanisms produce a constant normal load between the traction drive rollers. This constant normal load must be sized to ensure adequate traction at the joint's maximum torque capacity. The obvious disadvantage of this constant normal load is that the traction drive rollers and their supporting bearings are needlessly overloaded during periods of low torque transmission. This constant normal load not only generates extra bearing losses at low torque transmission but, more importantly, shortens the drive systems fatigue life [3]. To ensure adequate traction with minimum friction loss, VLMs were developed. These mechanisms produce varying normal loads between the traction rollers that are proportional to the transmitted torque [4]. Two VLMs have been incorporated into the traction drive differential. These VLMs are known as the input VLM and the output VLM.

The input VLM produces a varying normal load between the input roller and the intermediate roller assembly. This mechanism consists of an upper thrust cam, a lower thrust cam, a thrust bearing, two radial bearings, a thrust bearing retainer, and four ball bearing balls, referred to as cam balls as shown in Figure 5. This mechanism generates a thrust force proportional to the input torque. This thrust force is applied to the input roller and is counteracted by the thrust bearing and bearing retainer. The radial bearings provide stability to the upper thrust cam. The upper and lower thrust cams are equipped with tapered contours that are formed by helical grooves. These contours contain cam balls as illustrated in Figure 6. Each contour is formed

by two helical grooves, one cut on a right-hand helix and the other cut on a left-hand helix. These two helical grooves converge at a depth that is slightly less than that of the cam ball radius (0.031 in.). A free-body diagram of the upper thrust cam and lower thrust cam is shown in Figure 7. The input torque (T_i) is transmitted from the upper thrust cam to the lower thrust cam by a compressive force generated in each cam ball. This compressive force F is normal to the tangent helical groove and is the resultant force of a horizontal force F_T and a vertical force F_L. Force F_T is the tangential force required to transmit the input torque T_i. Force F_L is a varying thrust load that is counteracted by the thrust bearing and bearing retainer shown in Figure 5. This varying thrust load is applied to the input roller and produces a varying normal load between the input roller and intermediate roller assembly.

The output VLM produces a varying normal load between the intermediate roller assembly and the pitch/yaw roller. This mechanism is incorporated into the intermediate roller assembly as shown in Figure 6. It consists of the intermediate drive roller, eight cam balls, and an intermediate transversing roller. These rollers contain tapered contours that work in conjunction with the cam balls in the same manner as the upper and lower thrust cams of the input VLM. As torque is transmitted between the intermediate drive roller and intermediate transversing roller, a thrust force F_L is generated that produces the varying normal force F_N.

The operational performance of the LTM was verified through testing during its preliminary design. A photograph of the test stand used is shown by Figure 8. The test stand was originally designed to accommodate two different types of speed reducers; a power hinge reducer, which was seen to be economically unfeasible; and a harmonic drive reducer, which is now being used. The test-stand differential is very similar to the LTM small-joint differential. Similar bearings and traction drive rollers are employed in both cases. The test stand is equipped with an input VLM and an output constant-loading mechanism. This arrangement provides the capability to compare the two different types of loading devices. Some of the parameters tested were the starting torque, back-driveability, mechanical efficiency, and torque capacity. The test stand demonstrated that a traction drive differential equipped with VLMs will satisfactorily transmit its designed torque capacity with a mechanical efficiency of $\sim$90 percent.

The starting torque of the test stand differential was measured for the pitch motion and yaw motion independently. The yaw motion involves only the input VLMs, while the pitch motion involves both the input VLMs and the output constant-loading mechanism. This allows comparison between VLMs and the constant-loading mechanism. To measure the starting torque of the pitch rotation, the yaw axis was fixed to the test stand base, and a torque watch was chucked to one input shaft of the differential (this shaft is also the input shaft of one input VLM) while the other input shaft was free to rotate. Similarly, to measure the starting torque of the yaw rotation, the pitch axis was locked, and torque was applied to one input shaft. Starting torque for the yaw rotation ranged from 65 oz-in. to 105 oz-in., and rotation in the

counterclockwise direction averaged 10 oz-in. less than the clockwise direction. The starting torque for the pitch rotation ranged from 16.5 to 27.75 oz-in. with no significant difference in the direction of rotation. The starting torque for the yaw rotation is much higher due to the constant-loading mechanism which is not involved in the pitch rotation. Therefore, the VLMs accounts for 25 percent of the total starting torque while the constant-loading mechanism accounts for 75 percent.

The spring constant of the test stand input VLM was also measured. To measure this spring constant the pitch/yaw roller and intermediate roller were removed from the differential housing. Next, a rigid bar (6 in. x 1.5 in. x 0.5 in. aluminum) was clamped to the driving roller and wedged against the wrist housing to prevent rotation of this roller. A large C-clamp was tightened over the end of the driving roller and the differential housing to prevent axial motion of the roller shaft. To measure the angular rotation, a rigid aluminum bar (1.5 in. x 0.5 in.) was clamped to the input shaft of the VLM and a dial indicator was located 6 in. along this bar from the shaft axis. To load the mechanism, a torque watch was chucked to the input shaft of the VLM. The applied torque was increased in 5 in.-lb increments, and three readings were recorded for each torque value. Data was taken for clockwise and counterclockwise rotations. The data was then plotted and linearized to determine the torsional spring constant of the mechanism. This spring constant was 1.3 in.-lb/min which is an order of magnitude smaller than the windup in the harmonic drive.

An important finding that was discovered from testing of the test stand was the inability of the input VLMs to satisfactorily produce loading and allow unloading between the driving roller and intermediate roller without modification to the differential. As the differential transmits a fluctuating torque, the input VLMs generate a thrust force that changes in magnitude. Compliance within the traction drive differential allows the drive roller to translate within the needle roller bearings as this thrust force (applied to the drive roller) changes in magnitude. A parasitic friction force is generated between the driving roller and needle roller bearing during this translation that counteracts loading in an increasing torque condition and unloading in a decreasing torque condition. The exact friction coefficient between the driving roller and needle roller bearings is unknown, making it impossible to calculate the exact value of this friction force. This friction force was originally estimated assuming a friction coefficient of 0.1. This estimate indicated that the driving roller would translate and satisfactorily produce loading and allow unloading between the driving roller and intermediate roller. It was discovered during testing that the friction coefficient was much higher than expected. This produced a higher friction force than calculated. During an increasing torque condition, the friction force counteracted loading to the extent that the driving roller would lose traction and slip. During a decreasing torque condition, the friction force counteracted unloading which caused the driving roller to remain loaded to the extent that it would hang. This hanging condition allowed the compression force generated in the cam balls of the input VLMs to diminish which caused lost motion between the upper and lower thrust cams of the input VLMs. To

correct this problem, a special linear ball bearing assembly was designed, fabricated, and installed between the driving roller and needle roller bearings as shown in Figure 5. The coefficient of friction between the drive roller and linear ball bearing assembly is much less than 0.1 which reduced the parasitic friction force and allowed satisfactory loading and unloading between the driving roller and intermediate roller.

Some of the limitations of LTM pitch/yaw joint that have been observed so far are compliance (wind-up experienced in the drive train) and backdriveability. Compliance is a result of deflection in the VLMs, traction drive rollers, and traction drive supporting bearings. Backdriveability is related to the rolling losses in the traction drive rollers and their supporting bearings. Both compliance and backdriveability are related to the initial preload of the traction drive rollers. Compliance can be decreased by increasing the initial preload, but unfortunately, the torque required to backdrive the LTM pitch/yaw joint is increased. At the time of this writing, final assembly of the LTM is underway and the exact values for compliance and backdriving torque are not known. The traction drive rollers of each LTM pitch/yaw joint have small preloads to accommodate low backdriving torque requirements and good teleoperator performance. Each joint can be backdriven by a torque that is less than 5 percent of its maximum torque capacity. Preliminary static load testing appears to indicate more compliance than expected at these small preloads. Compliance can be reduced in future designs by increasing the stiffness of the traction drive rollers' mounting arrangement and the VLMs. The mounting arrangement of the traction drive rollers can be improved by incorporating angular contact bearing assemblies directly into the pitch/yaw roller, intermediate roller assemblies, and their supporting "T" shaft. These traction drive rollers and their supporting "T" shaft could be equipped with mating groves that contain bearing balls to create an angular contact bearing arrangement. This arrangement would allow the use of larger bearing balls than the commercial bearings that are presently used. Stiffness of the VLMs can be improved by increasing the number and size of the cam balls. Tapered rollers could also be used as an alternative to the spherical cam ball presently being used.

Future development of the LTM pitch/yaw joint should include thermal vacuum testing. Several concerns must be investigated such as galling of the traction drive rollers in a vacuum environment and effect of temperature change on the preload. Different plating materials and processes should be evaluated to determine their lubricating performance for the traction drive differential. Additional capabilities should be incorporated into the VLMs such as remotely adjustable and temperature compensating preloads.

CONCLUSIONS

A joint mechanism for a space telerobot was developed for NASA Langley Research Center. This joint mechanism incorporates a traction-drive differential that is equipped with variable preload mechanisms. It meets the requirements of both teleoperators and robots. Backlash is eliminated and high stiffness is provided that accommodates accurate and rapid positioning

needed in robots; and low friction and inertia is obtained to minimize operator fatigue needed in teleoperated manipulators. By meeting the requirements of teleoperated manipulators and robots, this joint mechanism is the first operational system to mechanically merge these two technologies into a "telerobot".

REFERENCES

1. Loewenthal, Stuart H., Rohn, Douglas A., and Steinetz, Bruce M.: Applications of Traction Drives as Servomechanisms. Presented at the 19th Aerospace Mechanism Symposium.

2. Anderson, William, Steinetz, Bruce M., and Rohn, Douglas A.: Evaluation of a High-Torque Backlash-Free Roller Actuator. Presented at the 20th Aerospace Mechanism Symposium.

3. Rothbart, ed. Mechanical Design and Systems Handbook - 1985, Loewenthal, Zaretsky, Traction Drives, Chapter 34, 1985.

4. Loewenthal, Stuart H., and Zaretsky, Erwin V.: Design of Traction Drives. NASA Reference Publication 1154, 1985.

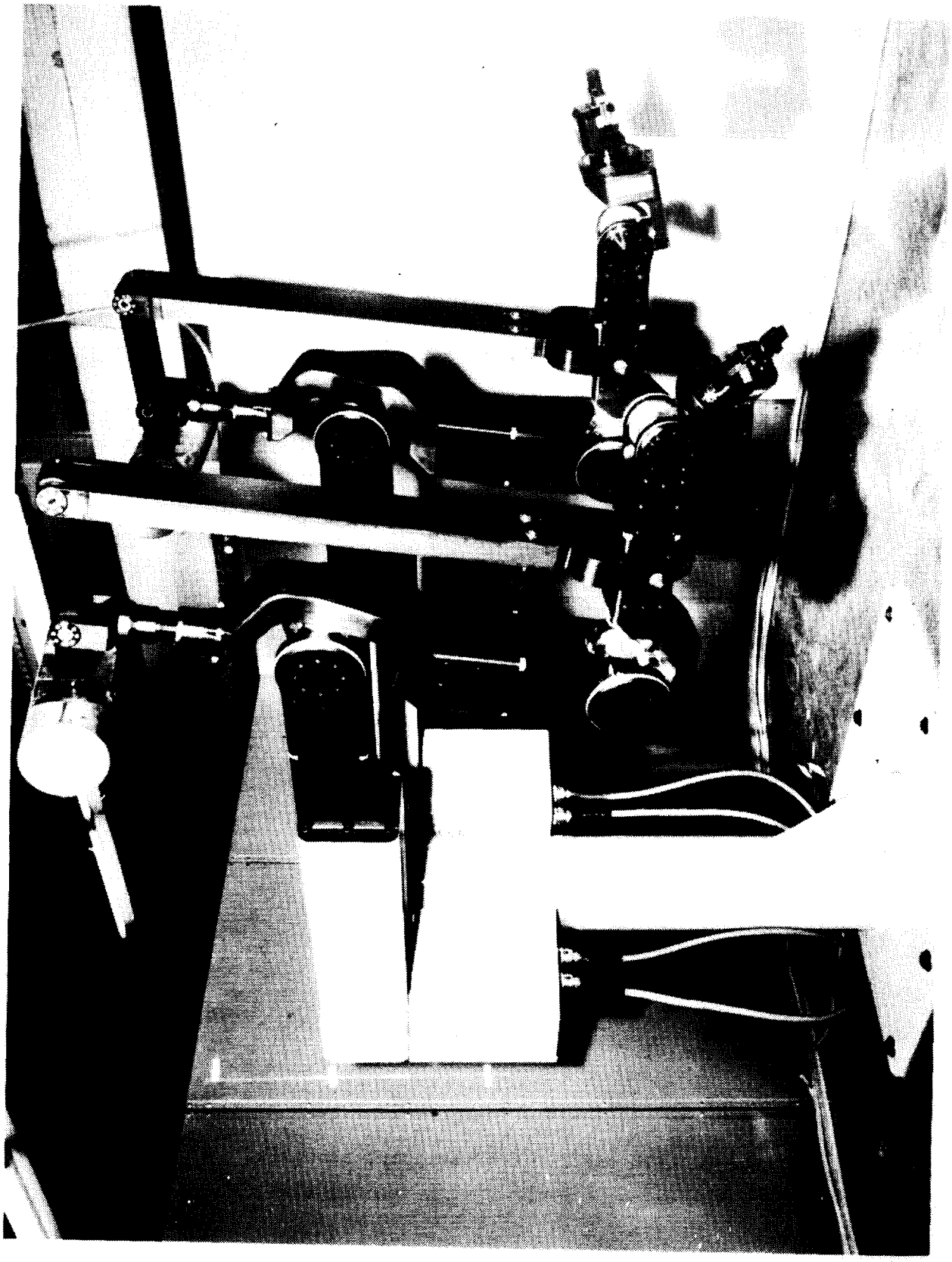

Figure 1. Laboratory Telerobotic Manipulator (LTM) slave.

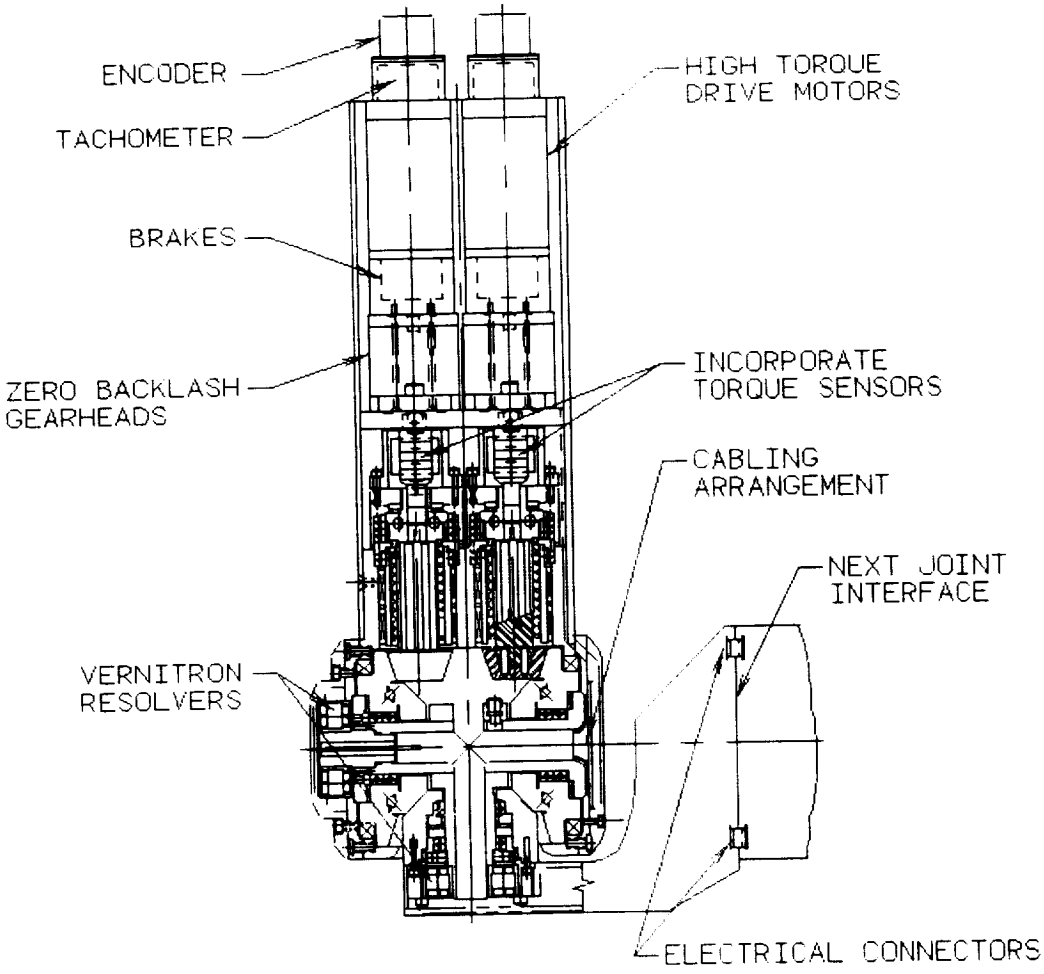

Figure 2. LTM small pitch/yaw joint assembly.

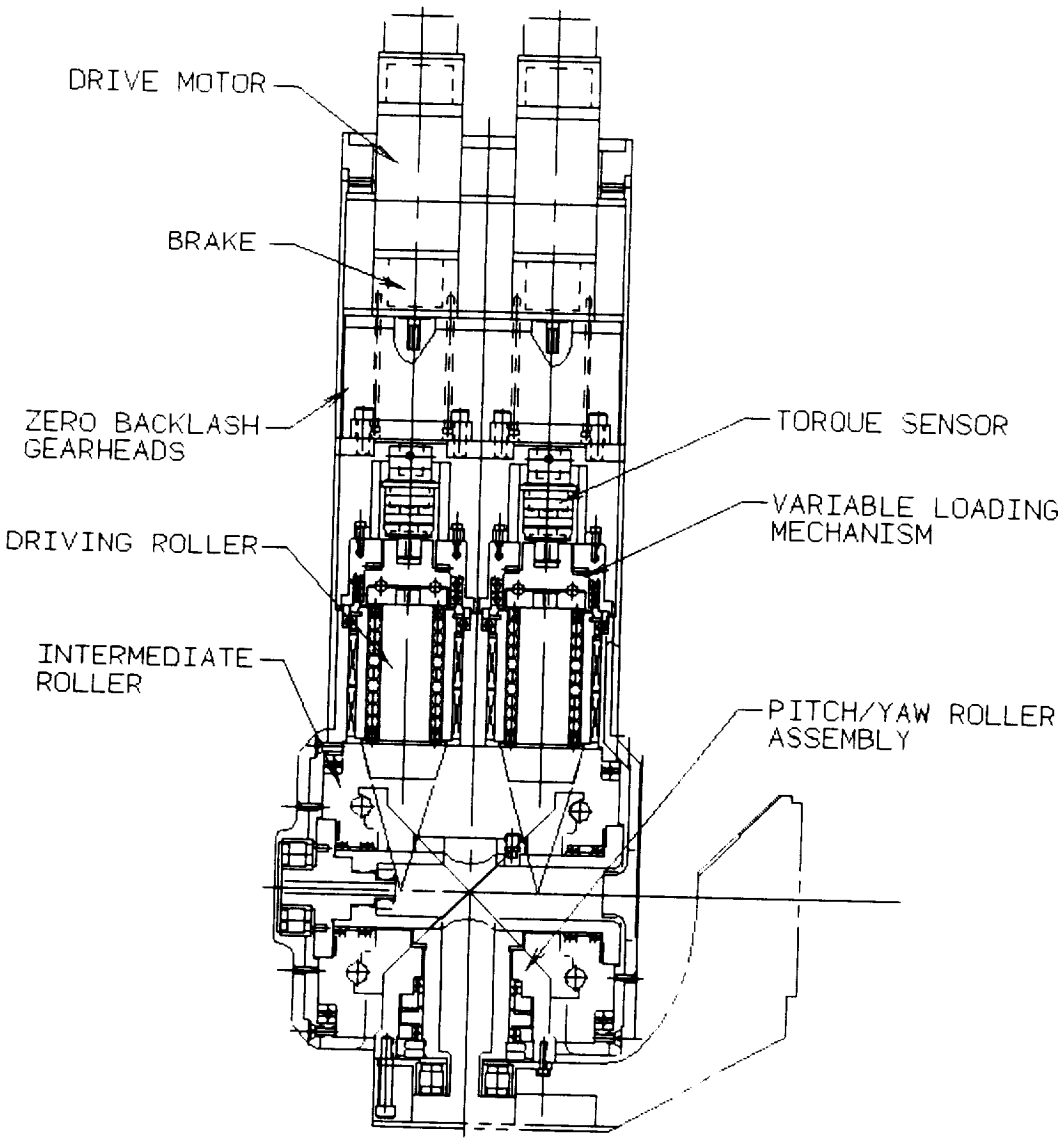

Figure 3. LTM large pitch/yaw joint assembly.

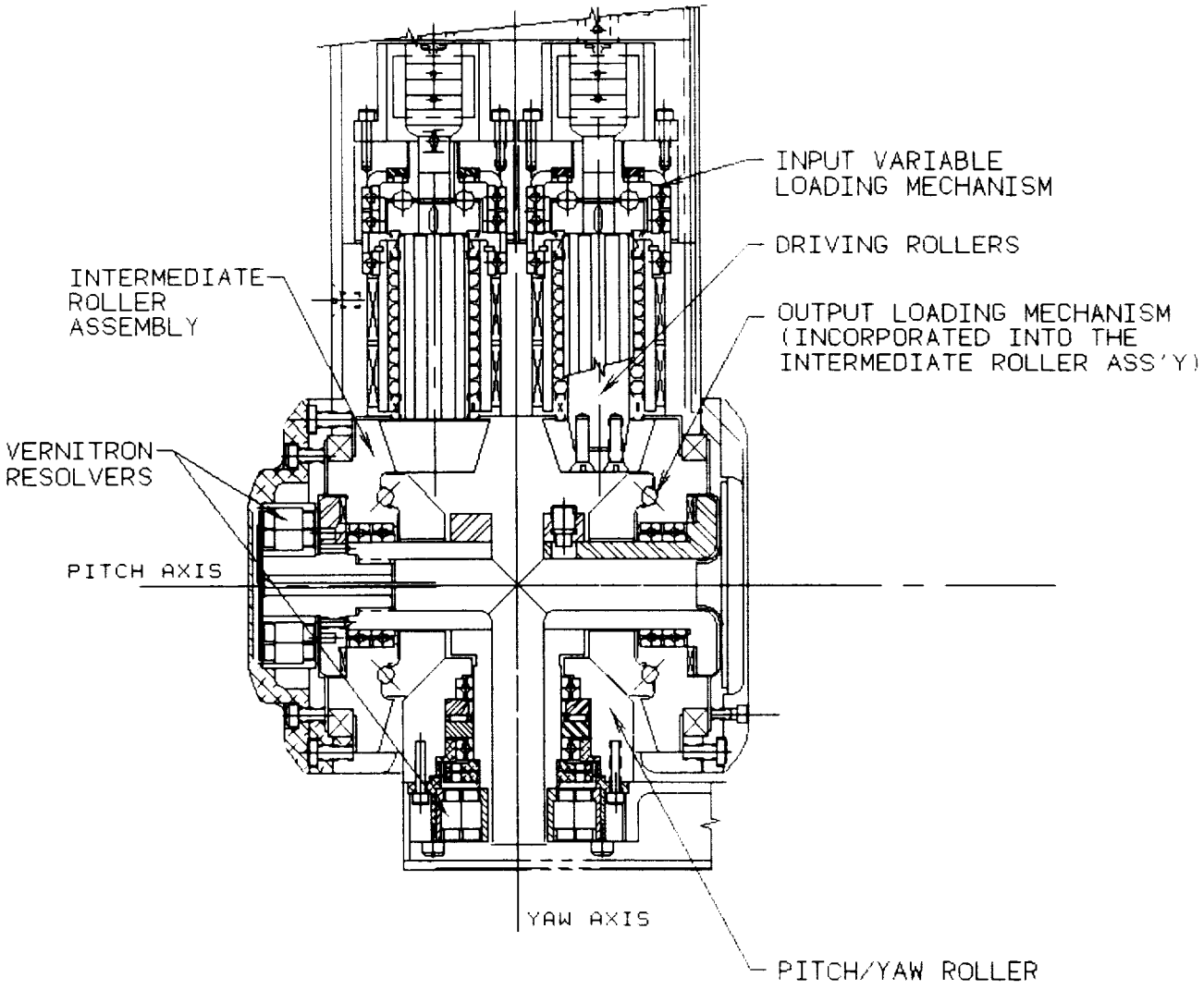

Figure 4. LTM traction drive differential.

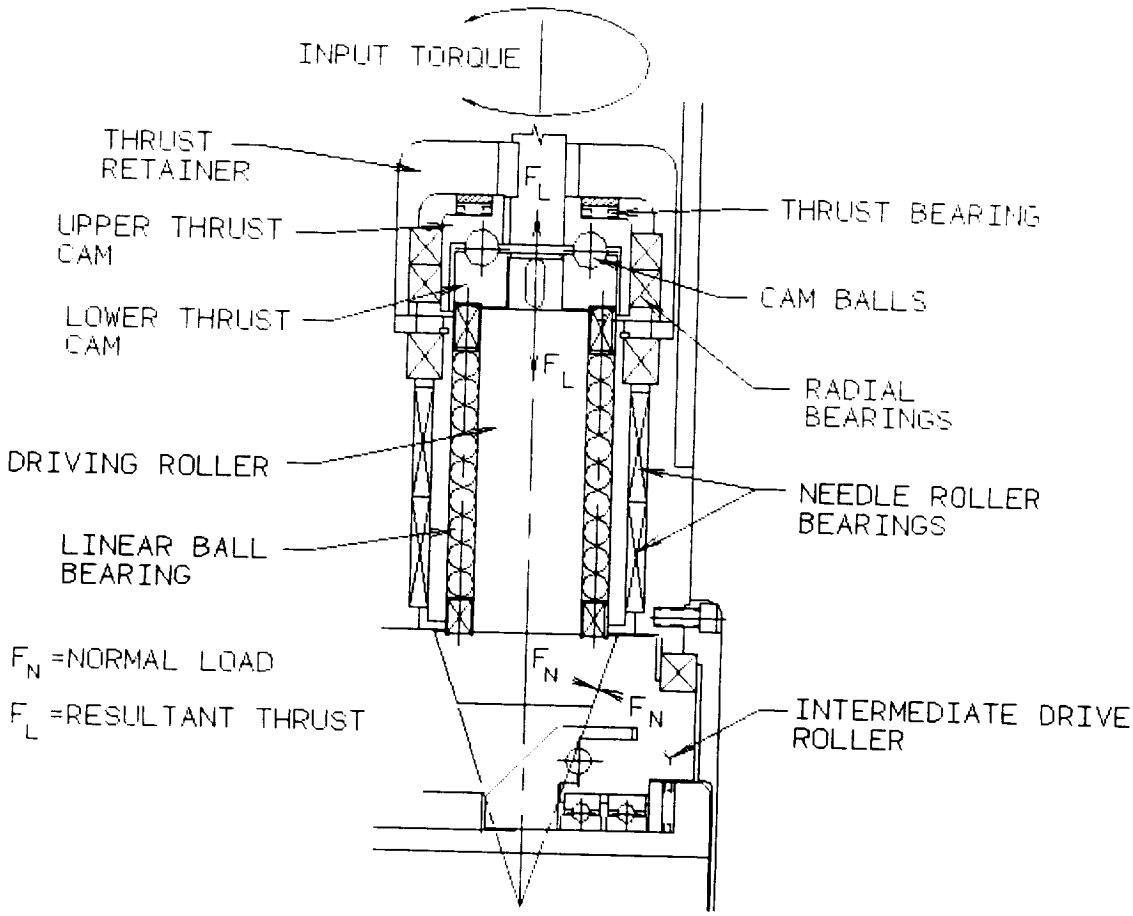

Figure 5. Input variable-loading mechanism.

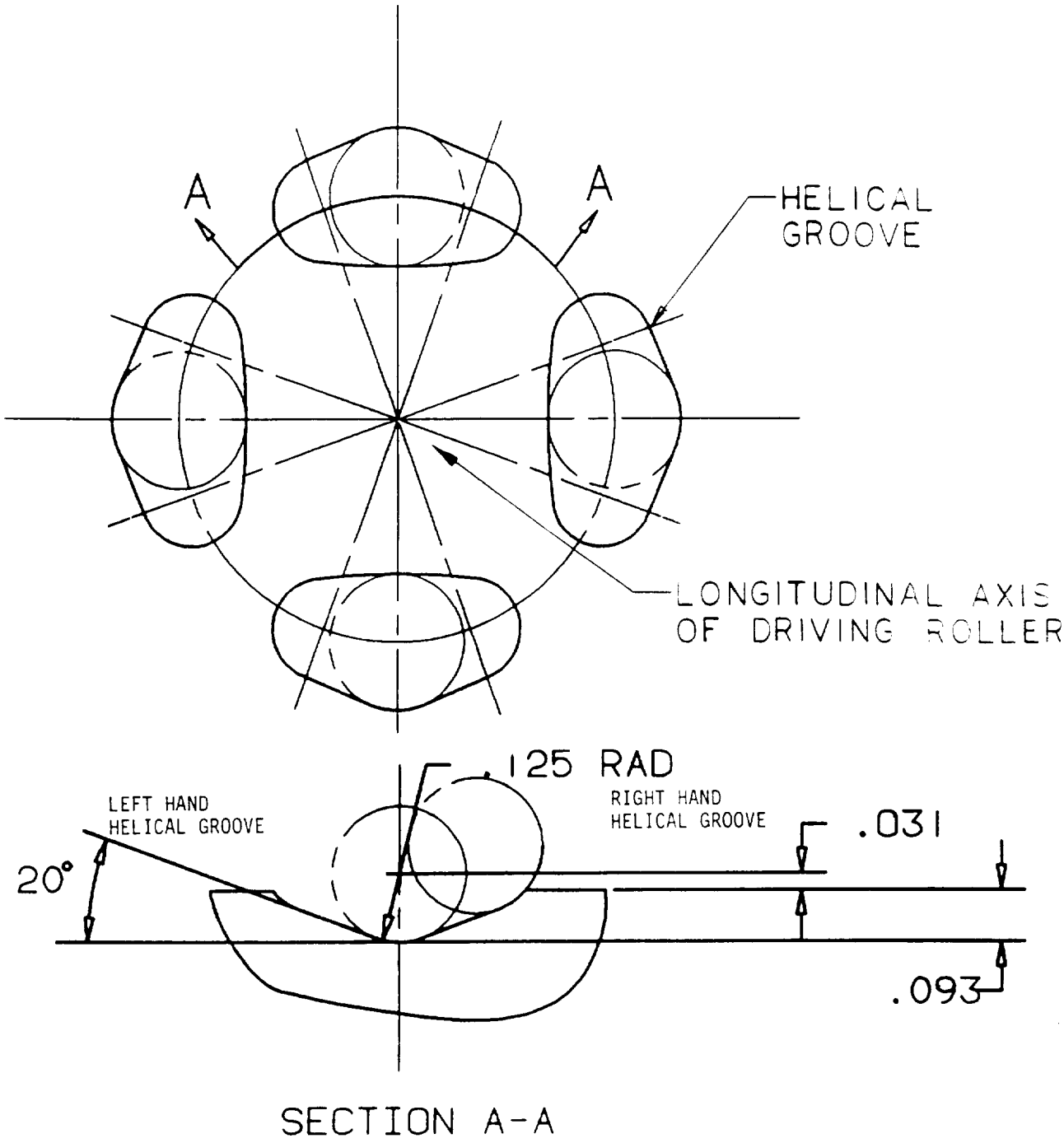

Figure 6. Thrust cam groove detail.

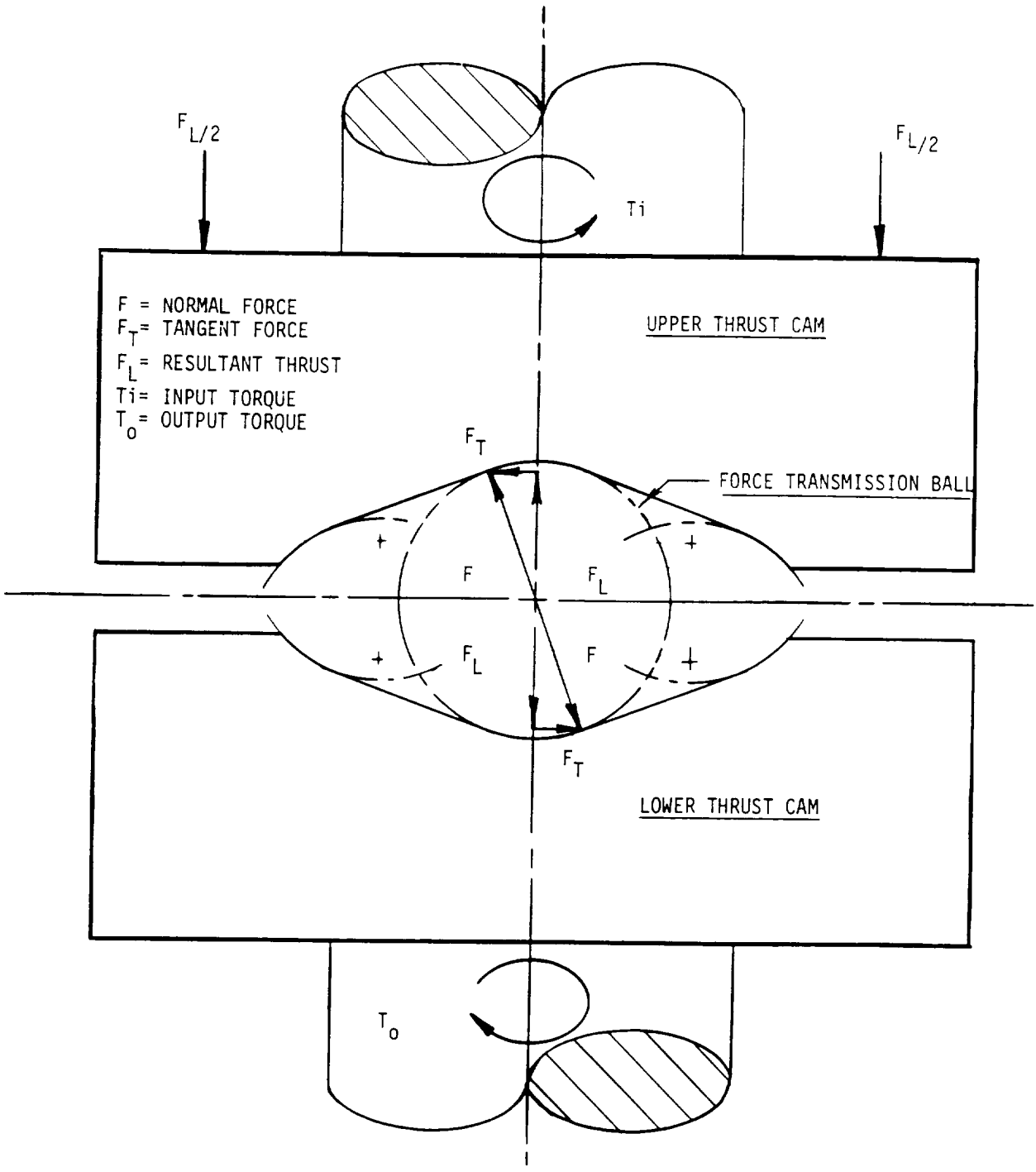

Figure 7. Free-body diagram of variable loading mechanism.

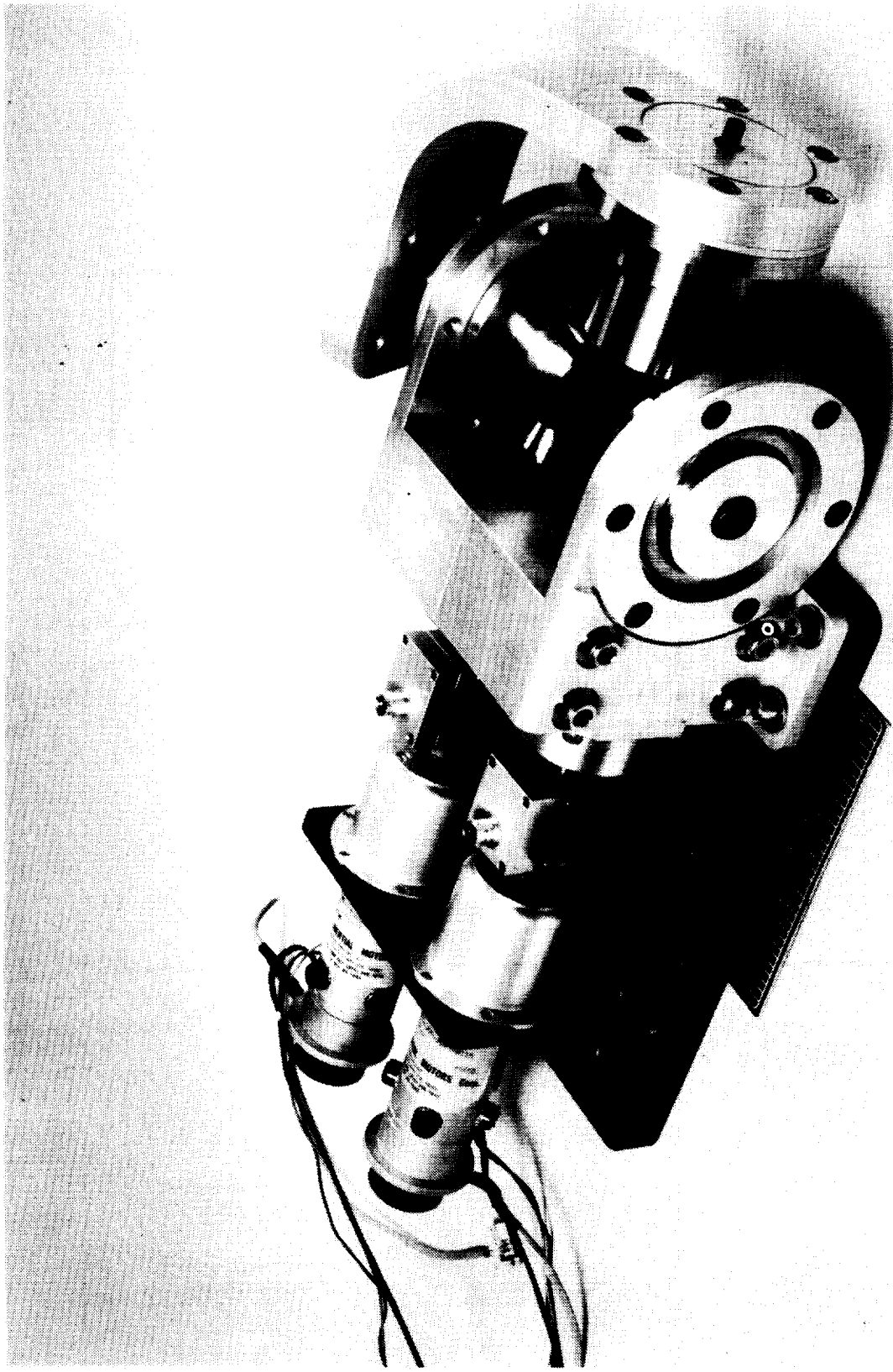

Figure 8. LTM test stand.